



increasing body of evidence suggests that the O-polysaccharide plays an important role in mediating bacteria–host interactions, such as effective colonization of the host and resistance to complement-mediated immune responses.<sup>7</sup>

The biosynthetic pathway of LPS has been studied extensively in the past few decades.<sup>2</sup> The current dogma is that LPS biosynthesis contains two separate pathways: Lipid A-core biosynthesis and O-polysaccharide biosynthesis. The lipid A-core structure is produced by sequentially transferring sugars onto the preformed lipid A on the cytosolic side of the inner membrane, which is then transported to the periplasm by an ATP dependent transporter MsbA.<sup>8,9</sup> Separately, O-polysaccharide biosynthesis starts with the sequential addition of monosaccharides onto undecaprenol phosphate (UndP) to form the O-repeating unit on the cytosolic face of the cytoplasmic membrane. These repeating units, once completed, are translocated by a flippase (*wzx*) to the periplasmic face of the membrane, where they are polymerized from the reducing end by a polymerase (*wzy*). Finally, the O-polysaccharide-PP-Und is ligated to the Lipid A-core in the periplasm to form the complete LPS, which is transported to the outer surface of the bacteria by an unknown mechanism.

The observation that bacterial O-polysaccharides play an important role in the stimulation of human blood group antibodies has been studied over the past several decades. One of the intriguing hypotheses, explored by Springer and co-workers during 1960s, suggested that naturally occurring anti-A and -B antibodies are raised in response to the constant enteric bacterial stimulation within the intestinal flora.<sup>10,11</sup> These studies demonstrated that a variety of Gram-negative bacteria showed blood group activities, among which *Escherichia coli* O86:B7 had high B blood group activity.<sup>10</sup> By using *E. coli* O86:B7 as a model bacterial strain, the immuno-

logical response of humans and germ-free chickens upon inoculation with *E. coli* O86:B7 was studied.<sup>12,13</sup> The resulting high titers of anti-blood group B antibody supported the hypothesis that bacteria stimulate human natural blood group antibody production. It was shown later that the strong blood group B activity of *E. coli* O86 resulted from the O-polysaccharide structure that resembles the blood group B antigen epitope.<sup>14</sup> The complete structure of the O-polysaccharide from serogroup O86:H2 was elucidated and confirmed the presence of blood group B antigen epitope in O-repeating unit.<sup>15</sup>

In this work, we report a new O-polysaccharide structure obtained from *E. coli* O86:K62:B7 (abbreviated as B7), which is different from the published structure. Interestingly, comparison of these two structures showed that they are derived from the same O-repeating unit via different polymerization sites on different sugar residues (Fig. 1). The immunochemical activity of these two forms of LPS toward anti-B antibody was then studied and compared. The different antibody binding affinities were explained via molecular modeling of the tetrasaccharide fragment that contains the blood group B epitope. This work thus introduces a good system to study bacterial O-polysaccharide biosynthesis, especially the polymerization mechanism.

## 2. Experimental

### 2.1. Bacterial strains and antibody

*E. coli* O86:K61:B7 (ATCC 12701) was obtained from American Type Culture Collection (Rockville, MD). *E. coli* O86:K62:H2 was kindly provided by Dr. Willie Vann of the FDA, Bethesda, MD. Commercially available IgM monoclonal anti-B antibody (obtained from

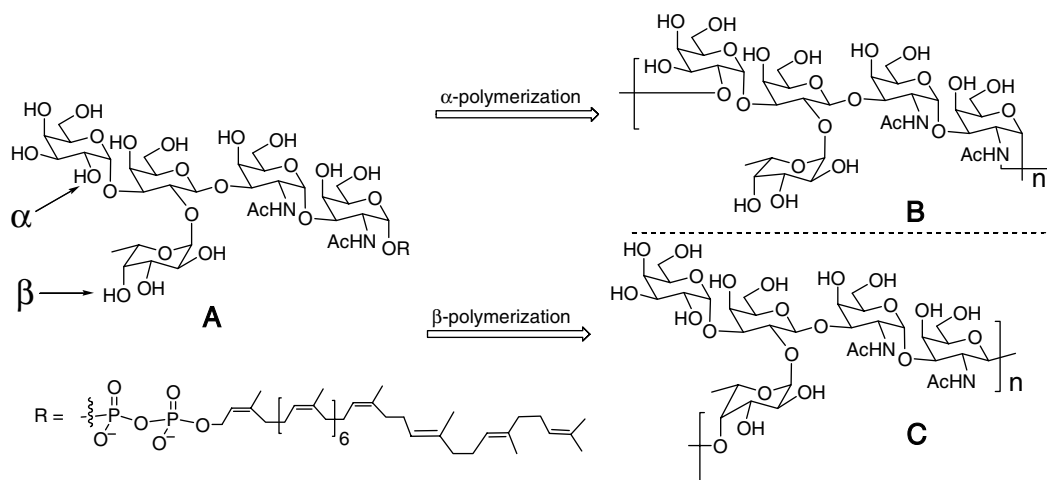


**Figure 1.** *E. coli* O86 O-antigen repeat unit and two O-polysaccharide structures: (A) O-repeat unit; (B) O-polysaccharide from *E. coli* O86:K61:B7; (C) O-polysaccharide from *E. coli* O86:K2:H2.

clone HEB-29) was purchased from Abcam Ltd. (Cambridge, UK).

## 2.2. Isolation of LPS and O-polysaccharide

Dried bacterial cells (20 g) were extracted with 50% (w/v) aqueous phenol (200 mL) at 65 °C for 15 min and then cooled to 4 °C, followed by low speed centrifugation (10,000g). The top aqueous solution was separated and dialyzed against distilled water until free from phenol. The clear solution was then lyophilized. The products were then dissolved in 0.02 M sodium acetate (pH = 7.0, 20 mL) and treated sequentially for 2 h each with DNase, RNase, and proteinase K at 37 °C. After removal of the precipitated materials, the solution was subjected to ultracentrifugation (110,000g, 4 °C, 12 h). The precipitated gels were then dissolved in distilled water and lyophilized to produce 1.2 g pure LPS. The LPS was degraded with aqueous 1% acetic acid at 100 °C for 1.5 h. The lipid precipitate was removed by centrifugation (12,000g, 30 min). The carbohydrate portion was purified on a Bio-Gel P2 column, and yielded 160 mg purified O-polysaccharide.

## 2.3. Structural determination of O-polysaccharide from *E. coli* O86:K61:B7

High-performance anion exchange chromatography (HPAE) was carried out on a Dionex CarboPack PA-10 (4 mm) anion exchange HPLC (HPAE) column with electrochemical detection on ED40 pulsed amperometric detector (PAD) followed by a PDR chiral optical rotation detector (ORD) connected in-line. Then 2 mg of the polysaccharide was hydrolyzed with trifluoroacetic acid (2 M) for 2 h at 100 °C. The retention times were compared to those of the standard monosaccharides: fucose, 2-amino-2-deoxy-galactose, 2-amino-2-deoxy-glucose, galactose, glucose, rhamnose, 2-amino-2-deoxy-mannose, mannose, and fructose. An optical rotation chromatogram was used for determination of absolute configuration of a given monosaccharide.<sup>34</sup>

For NMR experiments, 30 mg of the O-polysaccharide was dissolved in 0.6 mL of 99.96% D<sub>2</sub>O after being lyophilized from 99.9% D<sub>2</sub>O. For the structure determination of the O86 O-polysaccharide repeating unit, a suite of standard NMR experiments was obtained including ge-DQF COSY, ge-TOCSY, NOESY, ge-HSQC and ge-HMBC all in phase sensitive modes acquired on Bruker DRX AVANCE spectrometer operating at 500 MHz <sup>1</sup>H frequency with cryoprobe detection. NOESY spectra were taken with mixing times of 80, 50, 30, and 15 ms and cross-peaks scored according to their integrated volumes as strong (s), medium (m) and weak (w). All spectra were taken at an elevated temperature of 50 °C due to dynamic properties of the polysaccharide. Data were processed with NMRPipe and NMRDraw

in Linux. The observed chemical shifts were referenced to internal acetone at 2.225 and 31.07 ppm for <sup>1</sup>H and <sup>13</sup>C, respectively.

Methylation analysis was done via GC-MS of partially methylated alditol acetates and was performed at the Complex Carbohydrate Research Center at The University of Georgia.

## 2.4. ELISA of LPS with anti-B antibody

The LPS from each *E. coli* strain (O86:B7, O86:H2, K12) was dissolved in PBS buffer pH = 7.5 and were coated onto flat-bottomed microtiter plates for 48 h at 4 °C at a concentration of 10 µg/mL. Then, 2% polyvinylpyrrolidone (PVP) in PBS buffer was used to block nonspecific binding for 3 h. The anti-B antibody described above was used in series dilution. ELISA end-point titers were determined as described,<sup>15</sup> employing a secondary antibody goat anti-mouse IgM conjugated to HRP (1:1000) (Sigma). The peroxidase substrate (3,3',5,5'-tetramethylbenzidine, Sigma) was used to develop the signal, which was monitored at 405 nm.

## 2.5. Molecular modeling of tetrasaccharide fragments

Molecular modeling of the O86 tetrasaccharide fragment was carried out to interpret the NOESY data. The structures were generated using Macromodel Version 7.0 and minimized in 10,000 cycles of Monte Carlo steps with the MM2 force field with a continuum solvent model for water. 6700 structure models with an energy under 50 kJ/mol above the global minimum were kept for the MC chain. The NOE data were then reconciled with the molecular models and scored as follows. Strong NOEs were assumed to be spaced at 2.4 Å, medium NOEs at 2.8 Å, and weak NOEs at 3.1 Å. The sum of the squared deviations for all NOEs ( $\chi$ NOE) was considered as the NOE score for each model.

## 3. Results

### 3.1. Structure determination of the O-polysaccharide from *E. coli* O86:K61:B7

Initial inspection of the NMR spectra of the B7 O-polysaccharide indicated disagreement in both the <sup>1</sup>H and <sup>13</sup>C spectra with the published *E. coli* O86:H2 structure by Andersson et al.<sup>15</sup> Because we had no reason to question either the NMR data or the structure determination reported by Andersson et al., we concluded that the O-polysaccharide we have isolated from B7 strain differed from that reported in the earlier study, which utilized a clinical isolate. Therefore, we treated this structure as unknown and carried out a full structural determination.

Representative HPAE chromatograms of the hydrolyzed O86 polysaccharide showed Gal, Fuc, and GalN in a ratio of 2:1:2, suggesting a carbohydrate composition identical to that of the reported structure. The optical rotation chromatogram indicated the absolute configurations of these residues are L-Fuc, two D-Gal, and two D-GalN.

The HSQC spectrum reveals five peaks in the anomeric chemical shift region between 5.5 and 4.5 ppm ( $^1\text{H}$ ) and 89–104 ppm ( $^{13}\text{C}$ ) suggesting there are five monosaccharide residues in the repeating subunit. We annotated the anomeric proton signals by letters A through E (Fig. 2). Both the  $^1\text{H}$  and  $^{13}\text{C}$  chemical shifts as well as the  $^1\text{H}$  coupling constants indicate that residues A–D are  $\alpha$ -anomers while residue E is a  $\beta$ -anomer. Complete  $^1\text{H}$  and  $^{13}\text{C}$  spectrum assignments were made by standard methods and the results at 50 °C are given

in Table 1. Examination of the  $^1\text{H}$  coupling constants was used to assign the stereochemistry of each of the five ring systems and the 6-deoxy-sugar was recognized by the characteristic chemical shift of the methyl group. The aminosugars were identified by the characteristic chemical shifts of C2. The methyl group signals at 2.04 and 2.12 ppm indicate that both amino sugars are N-acetylated. We therefore identify the sugars residues as  $\alpha$ -Galp (A),  $\alpha$ -Fucp (B),  $\alpha$ -GalpNAc (C and D), and  $\beta$ -Galp (E) in agreement with the HPLC data. HMBC spectra were used to confirm the assignment given in Table 1, which accounts for all the magnetization observed in the HSQC spectrum (Fig. 2).

Methylation analysis shows the presence of five components, namely, 4,6-di-*O*-methyl-galactose, 3,4,6-tri-*O*-methyl-galactose, 2,3,4-tri-*O*-methyl-fucose, 2-deoxy-2-*N*-methylacetamido-4,6-di-*O*-methyl-galactose, and

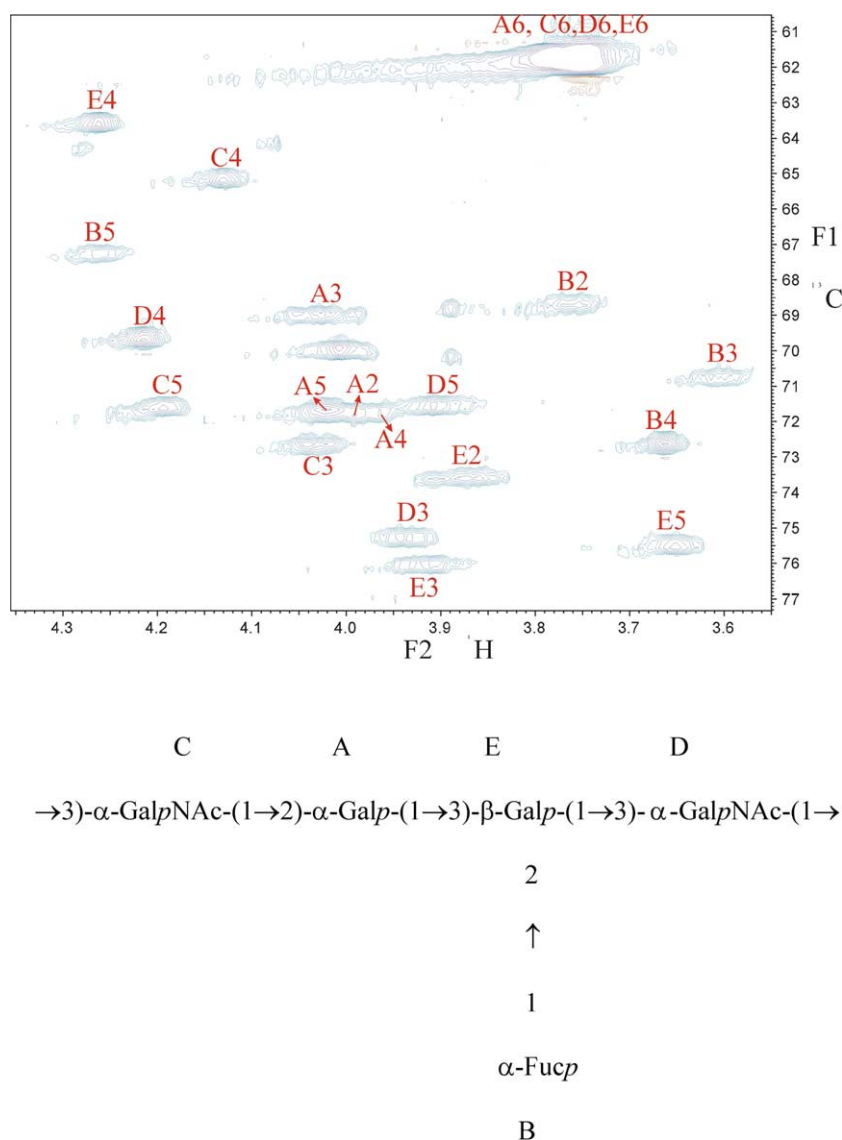


**Figure 2.** HSQC spectra of the *E. coli* O86:B7 O-polysaccharide. The anomeric protons are annotated by letters A through E.

**Table 1.** Chemical shift assignments for the O-polysaccharide of the *E. coli* O86:K61:B7 strain

O86	H-1 C-1	H-2 C-2	H-3 C-3	H-4 C-4	H-5 C-5	H-6 C-6	NHCOCH <sub>3</sub>
A— $\alpha$ -D-Galp	5.447 90.1	3.99 72.3	4.04 69.3	4.01 70.3	4.19 71.9	3.76 62.3	
B— $\alpha$ -L-Fucp	5.308 99.8	3.76 69.0	3.605 71.1	3.66 73.0	4.27 67.7	1.15 16.4	
C— $\alpha$ -D-GalpNAc	5.232 94.8	4.43 48.7	4.03 73.0	4.13 65.6	4.02 71.9	3.76 62.3	2.12 23.7
D— $\alpha$ -D-GalpNAc	5.066 94.0	4.215 49.8	3.94 75.6	4.22 69.9	3.91 71.9	3.76 62.1	2.04 23.1
E— $\beta$ -D-Galp	4.693 103.5	3.86 74.0	3.925 76.5	4.27 63.9	3.65 75.8	3.76 61.9	

2-deoxy-2-*N*-methylacetamido-3,4,6-tri-*O*-methyl-galactose in the ratio of 1.0:1.0:1.0:1.4:0.4.

The glycosidic linkage positions of residues B, D, and E are readily apparent from the HMBC data (Table 2). The NOE data (Table 3) are likewise in accordance with the assignments of residues B–E as  $\alpha$ -Fucp-(1→2)- $\beta$ -Galp, of residues E–D as  $\beta$ -Galp-(1→3)- $\alpha$ -GalpNAc and residues D–C as  $\alpha$ -GalpNAc(D)-(1→3)- $\alpha$ -GalpNAc(C). The anomeric proton of residue A shows a weak HMBC cross-peak to C3 of residue E as well as a strong NOE to H4 and a weaker NOE to H3 of residue E. This pattern of a strong NOE to an equatorial proton adjacent to the linkage position is characteristic of this stereochemical configuration and has been reported in previous studies of NOE's in the blood group B oligosaccharide.<sup>16</sup> We can therefore assign the linkage of A–E as  $\alpha$ -Galp-(1→3)- $\beta$ -Galp. This interpretation of the NOE data is confirmed by our molecular modeling study described below.

The HMBC as well as long-range single quantum correlation data do not give unambiguous evidence of the linkage of residue C. The anomeric proton of C shows cross-peaks only with the C3 and C5 of that residue and no other signals. The anomeric carbon signal shows no cross-peaks. Strong NOE peaks are seen between CH1 and AH1, AH2, EH2, and EH4 suggesting that

residue C is linked to either residue A or E. The clearest indication of the exact position of this linkage comes from methylation analysis, which is consistent with the linkages B1–E2, C1–D3, D1–E3, and A1–E3. These assignments account for all the methylation analysis except for the 2-linked Galp residue. Because the 2,3 substituted Galp is accounted for by residue E, we assigned the 2-substituted Galp as residue A. The linkage C–A as  $\alpha$ -GalpNAc-(1→2)- $\alpha$ -Galp is further supported by the strong NOE between CH1 and AH1, a characteristic pattern of NOE to an equatorial proton adjacent to the linkage position. A less prominent NOE is observed between CH1 and AH2, the linkage position. This assignment is also confirmed by our molecular modeling analysis below.

The structure reported in this work for *E. coli* O86:B7 strain differs from the reported structure in the linkage position and anomeric configuration of a single residue GalpNAc (residue C in our designation). In our structure (Fig. 2), this GalpNAc residue is in an  $\alpha$ -(1→2) linkage to the  $\alpha$ -Galp (A) residue whereas in the published structure, that GalpNAc is linked  $\alpha$ -(1→4) to  $\alpha$ -Fucp (B).

### 3.2. Two forms of LPS display different binding affinities with anti-blood group B antibody

In the B7 O-polysaccharide, the  $\alpha$ -linked Galp residue is part of the polysaccharide backbone, in which its C2–OH has been substituted with a GalpNAc residue. This C2–OH position was demonstrated by Lemieux et al.<sup>17</sup> to be critical for the binding of the anti-B antibody to the blood group B antigen. Therefore, it is envisaged that the LPS produced from these two *E. coli* O86 strains would display different binding affinities with anti-B antibodies. To confirm this hypothesis, an LPS ELISA assay was carried out. *E. coli* K12, which has no reported blood group activity, was used as a negative control. Antibody titration (Fig. 3) showed that the anti-serum had an end-point titer of ~1600 against *E. coli*

**Table 2.** HMBC peaks indicating glycosidic linkages

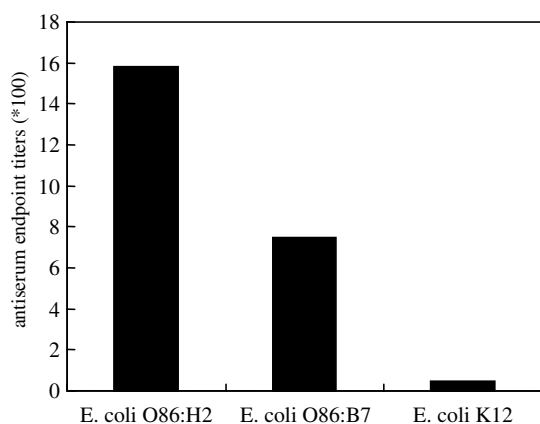
	<sup>1</sup> H and <sup>13</sup> C chemical shifts	proton– carbon pair
Anomeric proton region	5.45, 76.5 (weak) 5.31, 74.0 (5.23, 72.3) <sup>a</sup> 5.07, 73.0	AH1→EC3 BH1→EC2 (CH1→AC2) <sup>a</sup> DH1→CC3
Anomeric carbon region	3.94, 103.5 3.86, 99.8 4.03, 94.0 (weak)	EC1→DH3 BC1→EH2 DC1→CH3

<sup>a</sup> Parentheses denotes peak from HMBC spectrum processed with linear prediction to improve the resolution in the indirect dimension.



**Table 3.** NOE data at 30 ms mixing time

Proton pair	Chemical shift	Volume	Intensity	Confirmed linkage
BH1–EH2	5.31–3.86	18.5	Strong	$\alpha$ -Fucp(B)-(1→2)- $\beta$ -Galp(E)
BH1–EH3	5.31–3.92	8.39	Medium	
BH5–EH1	4.27–4.69	6.15	Medium	
AH1–EH3	5.45–3.93	2.45	Weak	$\alpha$ -Galp(A)-(1→3)- $\beta$ -Galp(E)
AH1–EH4	5.45–4.27	34.2	Strong	
AH5–EH3	4.19–3.93	92.8	Extremely strong (overlap)	
BH1–AH3	5.31–4.04	16.8	Strong	
BH1–AH5	5.31–4.19	5.59	Medium	
EH1–DH3	4.69–3.94	25.9	Strong	$\beta$ -Galp(E)-(1→3)- $\alpha$ -GalpNAc(D)
AH1–CH5	5.45–4.02	6.55	Medium–weak	
CH1–EH2	5.23–3.86	48.8	Strong	
CH1–EH4	5.23–4.27	24.6	Strong	
CH1–AH1	5.45–5.23	15.6	Strong	
CH1–AH2	5.23–3.99	26.7	Strong	$\alpha$ -GalpNAc(C)-(1→2)- $\alpha$ -Galp(A)
DH1–CH4	5.07–4.13	23.6	Strong	$\alpha$ -GalpNAc(D)-(1→3)- $\alpha$ -GalpNAc(C)
DH1–CH3	5.07–4.03	35.0	Strong	

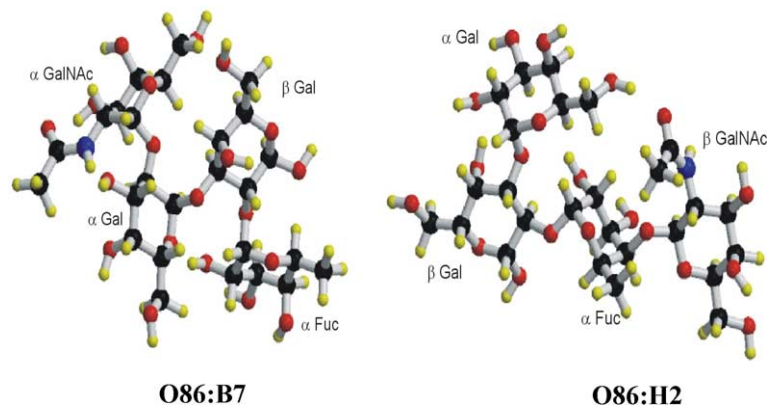
**Figure 3.** ELISA end-point titers of anti-blood group B antibody with LPS.

O86:H2 LPS, which is consistent with a previous study.<sup>15</sup> The end-point titer against B7 LPS was twofold lower, that is, ~800. These results showed that the H2 strain possessed higher blood group B reactivity com-

pared to the B7 strain, and further confirmed the critical role of the C2–OH of the  $\alpha$ -linked Galp residue in the blood group B epitope (Fig. 4).

### 3.3. Molecular modeling of tetrasaccharide fragments from two O-antigen structures

Molecular modeling of a tetrasaccharide fragment (residues A, B, C, and E) from the proposed B7 O-polysaccharide structure was carried out. The NOEs predicted for each model was compared with that measured for the polysaccharide using 30 ms mixing times (Table 3). Each molecular model in the Monte Carlo chain was scored following the rules given in the Experimental Section and the penalty scores were plotted as a function of glycosidic dihedral angles along with the calculated energies. The models with the lowest values of NOE penalty are those with the lowest energy, especially for the residues of the blood group B trisaccharide composed of residues A–E–B. This result is in agreement with a relatively rigid single conformation for the blood group B trisaccharide, which has been proposed by

**Figure 4.** Molecular modeling of tetrasaccharide fragments of O-polysaccharides from *E. coli* O86:B7 and O86:H2 strains.

**Table 4.** Glycosidic dihedral angles of the lowest energy tetrasaccharide model following the IUPAC heavy-atom convention

Linkage	$\Phi$	$\Psi$
C–A2	72.3	79.6
A–E3	66.6	–179.4
B–E2	–68.2	148.1

NMR, X-ray crystallographic, and molecular modeling studies.<sup>16,18</sup> The conformation of  $\alpha$ -GalpNAc-(1→2)- $\alpha$ -Galp linkage between residues C–A has not been previously studied and, although our data indicate it may not be a single rigid conformer, the results do confirm the strong NOE between CH1 and AH1, which is caused by a very short distance between these two protons in the lowest energy model (2.167 Å, Table 4). While the distance between CH1 and AH2 (2.723 Å) matched the NOE data well, some other NOE values are not well predicted by the single low energy model suggesting that some other conformers must contribute to the conformation of this linkage.

#### 4. Discussion

LPS heterogeneity is mostly found in the structural diversity of O-polysaccharide. The variations of O-antigens within one bacterial species can be exerted at different levels, such as nonstoichiometric modifications of polysaccharide backbones with glucosyl and fucosyl residues, change of anomeric linkages of the O-PS repeating unit, and change of major range of polysaccharide chain length.<sup>19</sup> A number of studies have been carried out to reveal the genetic basis of O-polysaccharide variations. Three possible mechanisms have been proposed.<sup>19</sup> These are lateral gene transfer followed by recombination, phage-induced conversion, and regulated expression of O-antigen biosynthetic genes. We report in this work the finding of a new O-polysaccharide structure from *E. coli* O86 serogroup. This new O-polysaccharide is structurally related to the previous reported structure in that both are derived from the same pentasaccharide repeating unit, but are polymerized from the same GalpNAc residue to different terminal residues (Gal and Fuc) via  $\alpha$  and  $\beta$  glycosidic linkages, respectively. The genetic basis of this structural difference is currently under investigation in our laboratory. The recent sequencing of O-antigen biosynthetic gene clusters of these two strains revealed that they have identical genetic sequence, including the *wzy* genes.<sup>21,33</sup> This finding is not surprising, because a similar phenomenon has been reported by Lam et al. in their study of serotype conversion of *P. aeruginosa* PAO1.<sup>20</sup> It was discovered that bacteriophage D3 was capable of lysogenizing *P. aeruginosa* PAO1 to change the glycosidic linkages between O-units from

$\alpha$ -(1→4) to  $\beta$ -(1→4) and acetylate FucpNAc sugar moieties. The *wzy* gene function in the host strain is inhibited by an  $\alpha$ -polymerase inhibitor and the phage-encoded  $\beta$ -*wzy* gene product forms the new  $\beta$ -linkage. Whether the serotype conversion of *E. coli* O86 in our case is related to the bacteriophage is currently unknown. The effort to elucidate the genetic mechanism is undertaken in our laboratory.

Currently, three major biosynthetic mechanisms have been proposed to describe the assembly and processing of O-polysaccharides of different structures.<sup>2</sup> They are the *wzy*-dependent pathway, the ABC transporter pathway and the synthetase-dependent pathway. The *wzy*-dependent pathway is involved in the synthesis of the majority of O-polysaccharides, especially heteropolymers. This process begins with the formation of the O-repeating unit from the cytoplasmic face of the inner membrane by different glycosyltransferases that are predicted to be soluble or peripheral membrane proteins. The completion of the O-repeating unit is followed by its translocation to the periplasmic side by *wzx*, where it is polymerized into polysaccharide by *wzy*. The chain length of polysaccharide is controlled by *wzz*. Recently, progress has been made in the study of O-repeating unit biosynthesis translocation. The in vitro expression of glycosyltransferases enables the successful reconstruction of O-repeating unit along its biosynthetic pathway.<sup>21</sup> A study by Valvano et al.<sup>22,23</sup> showed that *wzx* can function independent of the O-repeating unit chemical structures. In contrast, the polymerization mechanism of the key step in O-polysaccharide biosynthesis has still remained elusive. The difficulty lies in the fact that: (1) *wzy* genes share little sequence homology, and the lack of conserved domain has complicated the identification of catalytic site and binding residues; (2) the structurally defined O-repeating unit substrate for polymerization is relatively difficult to obtain; (3) a sensitive polymerization assay is yet to be developed. Therefore, the study of the *wzy* polymerization mechanism has largely lagged behind. Our finding in this work, that two different O-polysaccharides could be derived from the same O-repeating unit, can potentially provide us a good system to facilitate the study of polymerization in detail. In combination with our recent successful reconstruction of *E. coli* O86 O-unit tetrasaccharide fragment, this finding suggests a method for elucidation of O-polysaccharide polymerization mechanism.

The blood group B reactivity of *E. coli* O86 comes from the presence of B antigen epitope in the O-polysaccharide structure. Despite the fact that the two forms of *E. coli* O86 polysaccharide share the same O-repeating unit, they display different binding affinities toward anti-B antibody, resulting from the different polymerizations. The structural difference of these two polysaccharides becomes more evident when we inspect the molecular models of two tetrasaccharide fragments,

which contain the B antigen epitope. In the model of the B7 tetrasaccharide, the  $\alpha$ -GalpNAc substitutes C2–OH of  $\alpha$ -Gal residue, blocking the access to the  $\alpha$ -Galp residue while leaving the  $\alpha$ -Fucp and  $\beta$ -Galp residues relatively free to react with the antibody. The model of the tetrasaccharide from strain H2 shows that the  $\beta$ -GalpNAc blocks access to the Fuc residue while leaving free access to both the  $\alpha$ -Galp and  $\beta$ -Galp residues. Previous studies in mapping the detailed combining sites of anti-B monoclonal antibodies with a panel of synthetic blood group B analogs<sup>17</sup> revealed that C2–OH on  $\alpha$ -Galp and C4–OH on  $\beta$ -Galp residues were key elements for antibody recognition, whereas the antibody could either partially or completely tolerate the deoxy forms of other hydroxyl groups. More recent characterization of recognition of blood group B trisaccharide derivatives by specific lectin also reached the similar conclusion.<sup>24</sup> The result of LPS ELISA study in this work is consistent with the above findings. We note that a number of bacterial species possess blood group reactivities.<sup>25–31</sup> Structural and immunological studies demonstrated that blood group activity was related to the cell surface carbohydrates that contain epitopes identical or similar to natural blood group antigens. What is remarkable is that any of those cell surface antigens can induce blood group antibodies when the terminal epitope of the blood group antigen is for the most part buried as an internal sequence of an O-antigen.<sup>32</sup>

In summary, we elucidated a new O-polysaccharide structure from *E. coli* O86:K61:B7. NMR spectroscopy analysis revealed that this O-polysaccharide has a distinct polymer structure compared to the structure previously obtained from *E. coli* O86:K2:H2 strain. The two polysaccharides share the same pentasaccharide repeating unit, but differ in the anomeric configuration of the linkage, the linkage position, and the identity of the residue through which the polymerization occurs. Molecular modeling of the tetrasaccharide fragments indicates that the structure differences account for the binding affinity of the two strains toward anti-blood group B antibody. This finding introduces a good system for the further study of O-polysaccharide biosynthesis mechanism.

### Acknowledgments

We thank Dr. Russell Carlson of the CCRC for methylation analyses. P. G. Wang acknowledges support from an endowed Ohio Eminent Scholar Professorship on Macromolecular Structure and Function in the Department of Biochemistry at The Ohio State University and financial support (R01 AI44040) from National Institutes of Health. C. A. Bush acknowledges the support MCB-02-12702 from The National Science Foundation.

### References

1. Luederitz, O.; Tanamoto, K.; Galanos, C.; McKenzie, G. R.; Brade, H.; Zaehring, U.; Rietschel, E. T.; Kusumoto, S.; Shiba, T. *Rev. Infect. Dis.* **1984**, *6*, 428–431.
2. Raetz, C. R. H.; Whitfield, C. *Annu. Rev. Biochem.* **2002**, *71*, 635–700.
3. Erridge, C.; Bennett-Guerrero, E.; Poxton, I. R. *Microbes Infect.* **2002**, *4*, 837–851.
4. Reeves, P. R. *FEMS Microbiol. Lett.* **1992**, *79*, 509–516.
5. Caroff, M.; Karibian, D.; Cavaillon, J.-M.; Haeflner-Cavaillon, N. *Microbes Infect.* **2002**, *4*, 915–926.
6. Rietschel, E. T.; Brade, L.; Schade, U.; Seydel, U.; Zaehring, U.; Brandenburg, K.; Helander, I.; Holst, O.; Kondo, S., et al. *Adv. Exp. Med. Biol.* **1990**, *256*, 81–99.
7. Skurnik, M.; Bengoechea, J. A. *Carbohydr. Res.* **2003**, *338*, 2521–2529.
8. Reyes, C. L.; Chang, G. *Science* **2005**, *308*, 1028–1031.
9. Dong, J.; Yang, G.; McHaourab, H. S. *Science* **2005**, *308*, 1023–1028.
10. Springer, G. F. *Angew. Chem., Int. Ed. Engl.* **1966**, *5*, 909–920.
11. Springer, G. F.; Wang, E. T.; Nichols, J. H.; Shear, J. M. *Ann. N.Y. Acad. Sci.* **1966**, *133*, 566–579.
12. Springer, G. F.; Horton, R. E.; Forbes, M. J. *Exp. Med.* **1959**, *110*, 221–244.
13. Springer, G. F.; Horton, R. E. *J. Clin. Invest.* **1969**, *48*, 1280–1291.
14. Kochibe, N.; Iseki, S. *Jpn. J. Microbiol.* **1968**, *12*, 403–411.
15. Andersson, M.; Carlin, N.; Leontein, K.; Lindquist, U.; Slettengren, K. *Carbohydr. Res.* **1989**, *185*, 211–223.
16. Otter, A.; Lemieux, R. U.; Ball, R. G.; Venot, A. P.; Hindsgaul, O.; Bundle, D. R. *Eur. J. Biochem.* **1999**, *259*, 295–303.
17. Lemieux, R. U.; Venot, A. P.; Spohr, U.; Bird, P.; Mandal, G.; Morishima, N.; Hindsgaul, O. *Can. J. Chem.* **1985**, *63*, 2664–2668.
18. Azurmendi, H. F.; Bush, C. A. *Carbohydr. Res.* **2002**, *337*, 905–915.
19. Lerouge, I.; Vanderleyden, J. *FEMS Microbiol. Rev.* **2002**, *26*, 17–47.
20. Newton, G. J.; Daniels, C.; Burrows, L. L.; Kropinski, A. M.; Clarke, A. J.; Lam, J. S. *Mol. Microbiol.* **2001**, *39*, 1237–1247.
21. Yi, W.; Shao, J.; Zhu, L.; Li, M.; Singh, M.; Lu, Y.; Lin, S.; Li, H.; Ryu, K.; Shen, J.; Guo, H.; Yao, Q.; Bush, C. A.; Wang, P. G. *J. Am. Chem. Soc.* **2005**, *127*, 2040–2041.
22. Marolda, C. L.; Vicarioli, J.; Valvano, M. A. *Microbiology* **2005**, *150*, 4095–4105.
23. Feldman, F.; Marolda, C. L.; Monteiro, M. A.; Perry, M. B.; Parodi, A. J.; Valvano, M. A. *J. Biol. Chem.* **1999**, *274*, 35129–35138.
24. Rempel, B. P.; Winter, H. C.; Goldstein, I. J.; Hindsgaul, O. *Glycoconjugate J.* **2003**, *19*, 175–180.
25. Furukawa, K.; Kochibe, N.; Takizawa, H.; Iseki, S. *Jpn. J. Microbiol.* **1972**, *16*, 199–204.
26. Kishi, K.; Iseki, S. *Jpn. J. Microbiol.* **1976**, *20*, 109–114.
27. Springer, G. F. *Microb. Toxins* **1971**, *5*, 39–90.
28. Springer, G. F.; Williamson, P.; Brandes, W. C. *J. Exp. Med.* **1961**, *113*, 1077–1093.
29. Springer, G. F.; Williamson, P.; Readler, B. L. *Ann. N.Y. Acad. Sci.* **1962**, *97*, 104–110.
30. Widmalm, G.; Leontein, K. *Carbohydr. Res.* **1993**, *247*, 255–262.



31. Ratnayake, S.; Widmalm, G.; Weintraub, A.; Medina, E. *C. Carbohydr. Res.* **1994**, *263*, 209–215.
32. Perry, M. B.; MacLean, L. L. *Carbohydr. Res.* **1992**, *232*, 143–150.
33. Guo, H.; Yi, W.; Song, J.; Zhang, W.; Wang, P. G. *Appl. Environ. Microbiol.* **2005**, *71*, 7995–8001.
34. Stroop, C. J. M.; Bush, C. A.; Marple, R. L.; LaCourse, W. R. *Anal. Biochem.* **2002**, *303*, 176–185.